



WEDNESDAY SLIDE CONFERENCE 2023-2024

Conference #23

17 April 2024

CASE I:

Signalment:

1.5 year-old neutered male domestic shorthair cat (*Felis catus*).

History:

The cat presented for signs of pain evolving over the last month. Palpation during the clinical examination localized the pain to the cervical vertebral spine. Cervical radiographs revealed a moth-eaten lesion involving the left part of C3. A CT scan identified a monostotic osteoproliferative lesion centered on the left pedicle of C3 and causing stenosis of the spinal canal. A benign primitive bone neoplasia was suspected. Decompressive hemilaminectomy was performed one month later. Post-operative CT scan showed residual compressive bone material at the surgical site. The animal's condition rapidly declined after surgery (stage IV cranial cervical myelopathy). Unfortunately, the cat became comatose and was maintained under artificial ventilation for a few hours before owners elected euthanasia.

Gross Pathology:

The left lamina of C3 was fractured and an entire fragment of bone was missing due to the hemilaminectomy procedure. The left pedicle of C3 showed a focal and poorly demarcated 1-1.5 cm osteoproliferative lesion with irregularly branching bone trabeculae giving a

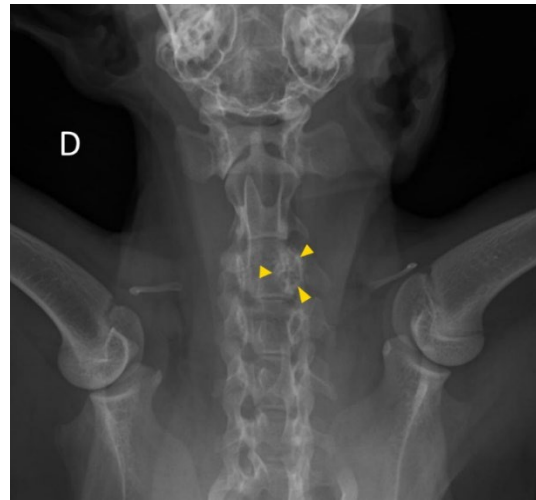


Figure 1-1. Vertebra, cat. Cervical radiographs revealed a moth-eaten lesion involving the left part of C3. (Photo courtesy of: Unité d'Histologie et d'Anatomie pathologique, Bio-Pôle Alfort, Département des Sciences Biologiques et Pharmaceutiques, Ecole Nationale vétérinaire d'Alfort (EnvA). <https://www.vet-alfort.fr/>).

spongy appearance. The spinal cord was dorsally displaced in the vertebral canal and a central focus of hemorrhagic myelomalacia was identified. The other organs were grossly unremarkable.

Microscopic Description:

Arising from the left pedicle of the C3 vertebra and protruding into the spinal canal and replacing the bone marrow is proliferative fibrovascular tissue that is poorly demarcated, moderately cellular and infiltrative. The tissue is composed of capillary and arteriole-type

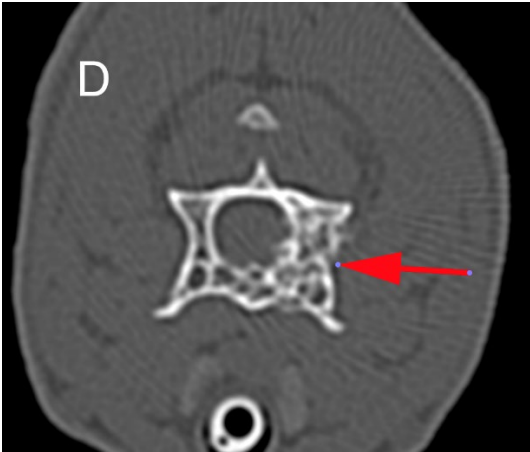


Figure 1-2. Vertebra, cat. CT scan identified a monostotic osteo-proliferative lesion centered on the left pedicle of C3 and causing a stenosis of the spinal canal.

vessels, and less often venule-like vessels, that irregular branch and grow within a loose, edematous and myxoid stroma. These vessels are lined by squamous and bland endothelial cells surrounded by pericytes (capillary-like vessels) or by a layer of smooth muscle cells (arteriole-like vessels). Atypias are minimal and no mitoses are observed. Some vessels are associated with small acute hemorrhages, fibrin exudation, or microthrombi. The surrounding trabecular bone shows bone remodeling characterized by irregular and scalloped outlines lined by plump osteoblasts and osteoclastic activity within Howship's lacunae.

The cervical spinal cord shows a dorso-lateral rotation around its longitudinal axis. Multiple foci of acute hemorrhagic necrosis/myelomalacia are seen within the grey and white matter, most likely secondary to the surgery. Some perivascular cuffs of neutrophils, macrophages and lymphocytes are identified nearby. Multifocally in the white matter, myelin sheaths are irregularly dilated and sometimes contain vacuolated macrophages indicative of Wallerian-like degeneration. Some ax-

ons are also severely dilated and form spheroids. These changes are most likely secondary to the spinal cord compression.

Contributor's Morphologic Diagnoses:

1. Cervical vertebra C3 (left pedicle): Vertebral angiomas (vascular vertebral malformation/hamartoma)
2. Cervical spinal cord: Myelomalacia, multifocal, acute, marked, with hemorrhages, axonal degeneration and spheroids.

Contributor's Comment:

Feline vertebral angiomas was first described in 1987 by Wells and Weisbrode in a case series of three cats. In this paper, the lesions were restricted to the thoracic vertebrae and diagnosed as an intraosseous vascular malformation.¹⁶

This entity is characterized by a focal proliferation of non-neoplastic blood vessels, hence the more recent denomination of vertebral angiomas.^{4,5,7,10,11,13-16} Similar histological lesions are recognized in human medicine with other names including skeletal angiomas, vertebral hemangioma, lymphangiomas, and hamartoma.^{7,16} This condition is not recognized as a true neoplasm because the



Figure 1-3. Vertebra, cat. The left lamina of C3 was fractured and an entire fragment of bone was missing (consequence of the hemilaminectomy). The left pedicle of C3 showed a focal and poorly demarcated osteoproliferative lesion.

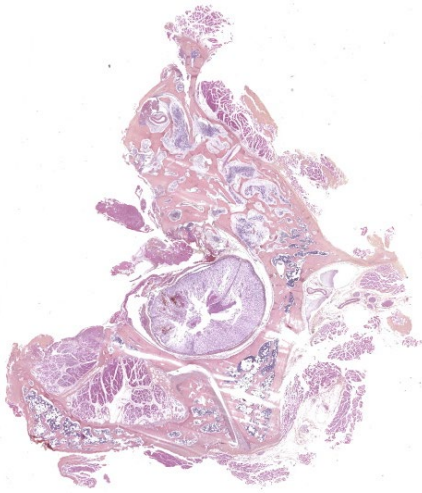


Figure 1-4. Vertebra, cat. One section of vertebra and spinal cord are submitted for examination. Part of the vertebral arch is missing as a result of hemilaminectomy. There is loss of marrow within the remaining vertebral arch. (HE, 3X)

vascular walls are well differentiated and are composed of multiple cell types, including pericytes, smooth muscle cells, and fibroblasts.^{7,10}

This condition is rare but is well described in the literature with 12 documented cases.^{4,5,7,10,11,13-16} Affected cats are typically young and less than 2 years old except for a 3.5 years old cat.^{4,5,7,10,11,13-16} No sex or breed predisposition have been reported. Animals present with a history, usually over 1 month, of chronic pain, lethargy, reluctance to walk, or progressive paraparesis.^{4,5,7,10,11,13-16} Most lesions are localized to the thoracic vertebrae but lumbar lesions have been described.^{4,5,7,10,11,14-16} They tend to originate from the vertebral arch, pedicle, or body and seem to spare the spinous process.⁷ Occasionally, they can involve multiple vertebrae, but no associated systemic vascular lesion has been observed.^{5,13} It is considered benign but can be locally aggressive.^{4,7,10,15} Our case is

original because it is the first report to our knowledge of cervical involvement. The clinical signs are likely caused by the spinal cord compression resulting from the expansion of angiomas into the spinal canal.

The diagnosis is first approached by imaging, mostly post-myelographic CT scan or MRI, in order to localize the lesion and evaluate the associated spinal cord compression.^{4,5,7,10,11,13-16} The differential diagnoses include vertebral new bone formation due to an old trauma, disc extrusion, bone abscess, granuloma, ancient hematoma or migrating foreign body.¹⁵ Neoplasia is less likely considering the young age of the affected animals, but lymphoma (especially in FeLV positive cats) or osteosarcoma should be considered.^{7,15}

The therapeutic approach is always surgical with a dual goal: 1) removing the spinal cord compression and 2) making biopsies for histopathological diagnosis.^{4,5,7,10,11,13-16} Cytologic imprints can be done during the surgery but are of poor diagnostic value.^{13,15} Adjuvant radiotherapy can be considered because of the potentially locally aggressive nature of the lesion and also because of the difficulty of complete resection in this area.^{7,11} Outcomes are variable. Some animals receiving surgery with or without radiotherapy are reported as free of disease over the following months or years.^{5,7,10} However, the surgery is not without risk, and relapse is also reported.^{4,15}

The pathogenesis of feline vertebral angiomas is still unclear. Because of the occurrence in young cats and the absence of an associated inflammatory or infectious process, developmental anomaly is currently considered most likely.^{7,10,11,16}

Histopathological features are consistent among all cases and are characterized by a

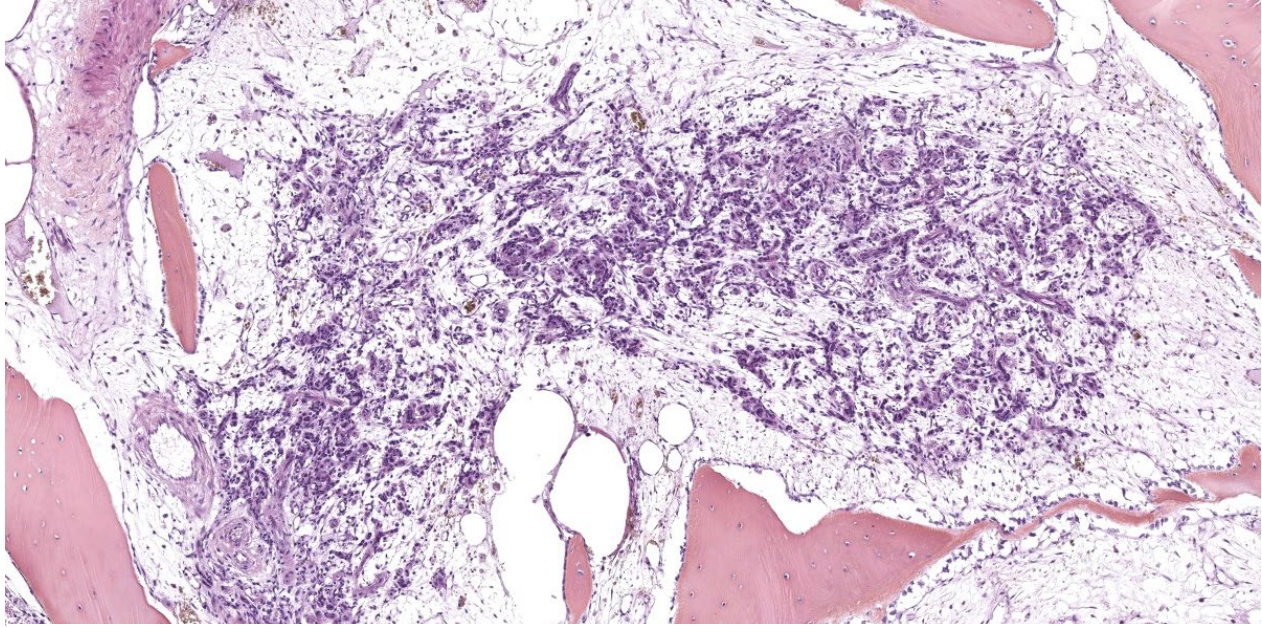


Figure 1-5. Vertebra, cat. Marrow spaces are devoid of marrow and contain plexiform proliferations of tortuous capillaries. (HE, 90X)

proliferation of rather well-differentiated capillaries, arterioles, and occasionally venules, into a loose and myxoid connective tissue with invasion of the spinal canal and the bone marrow, as well as bone remodeling and new bone formation.^{4,5,7,10,11,13-16}

Other type of angiomas have been reported in the cat, affecting the skin, cerebrum, meninges, and lungs.^{1-3,8,9}

Contributing Institution:

Unité d’Histologie et d’Anatomie pathologique
 BioPôle Alfort, Département des Sciences
 Biologiques et Pharmaceutiques
 Ecole Nationale vétérinaire d’Alfort (EnvA)
<https://www.vet-alfort.fr/>

JPC Diagnoses:

1. Vertebra, pedicle and body, hemi-laminectomy site: Angiomas, focally extensive, marked, with reactive osteolysis and osteoproliferation (bone modeling).
2. Cervical spinal cord, gray and white matter: Myelomalacia, diffuse, severe, with hemorrhage and axonal degeneration.

JPC Comment:

The contributor provides an excellent overview of this enigmatic condition that, until recently, had only been reported in young cats. Earlier this year, however, vertebral angiomas was reported in a three year old female intact Cavalier King Charles Spaniel who presented for ataxia and paraparesis.⁶ CT revealed osteolysis of the vertebral body and pedicles of T5 with compressive extradural material within the spinal canal. The dog was treated surgically with a dorsal hemilaminectomy and histopathologic samples collected intraoperatively were consistent with vertebral angiomas.⁶

Vertebral angiomas are one member of a cohort of non-neoplastic vascular malformations beset by confusing terminology, overlapping histologic features, and uncertain pathogenesis. Angiomas (also known as hemangiomas) has two microscopic patterns: either a mixture of blood vessel types, some of which can be cavernous, or a predominance of capillaries. Lobules of mature adipose tissue characteristically accompany the vascular elements.¹²

In addition to the vertebral angiomas so nicely discussed by the contributor, angiomas have been identified within the skin and subcutis of cats and dogs and in the skin of cattle. Calves have a reported generalized pattern of angiomas in which the heart, lungs, kidneys, and an assortment of other organs are involved.¹² There is a single case report of cerebral angiomas in a young cat presenting with generalized seizures, the clinical manifestation of bilateral nests of differentiated capillaries within the cerebral gray matter.¹²

Human and veterinary medicine is rich with various other hamartomatous vascular conditions, including meningoangiomas, angiomas, and arteriovenous malformations, the parsing of which requires equal measures of stamina and will. An excellent 2021 comparative review of proliferative vascular disorders in the central nervous system is a helpful reference for those attempting to understand the nuances of these difficult diagnoses.¹²

Our moderator this week was Dr. Julie Engiles, Professor of Pathology at the University of Pennsylvania School of Veterinary Medicine. Dr. Engiles began discussion of this case with a review of vertebral anatomy and by noting the important structures, such as the vertebral artery, that can be used as orientation

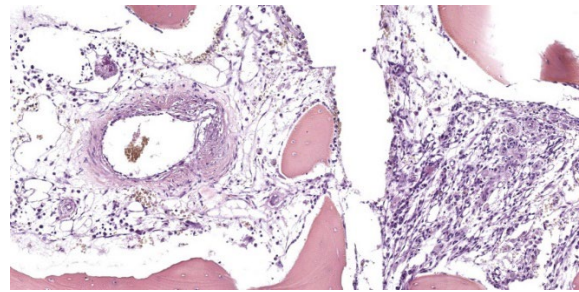


Figure 1-6. Vertebra, cat. Arterioles (left) within areas of vascular proliferation have asymmetric fibrosis of the smooth muscle wall and adventitia. (HE, 90x)

landmarks on this challenging slide. Dr. Engiles also stressed the importance of a collaborative approach among pathologists, radiologists, and clinicians in cases like this, where locating and appropriately sampling the lesion would be difficult without the insight provided by other members of the medical team. In this case, the lesions presented radiographically with an aggressive, moth-eaten appearance which provides helpful context for the relatively bland histologic appearance of the proliferative cells.

Immunohistochemically, the vascular markers Factor VIII and ERG helped to visualize the disorganized proliferation of vascular elements, while smooth muscle actin highlighted the smooth muscle in the proliferating vessel walls. Dr. Engiles noted that the proliferation of multiple cell types, including endothelial smooth muscle myocytes, and pericytes, supports the nonneoplastic classification of this entity, as neoplasia is typically characterized by the aberrant proliferation of a single cell type. The moderator noted that this lesion is sometimes called a hamartoma, which seems to connote an indolent, static process at odds with the typically proliferative and infiltrative behavior of these lesions. For this reason, the moderator prefers the more dynamic term angiomas.

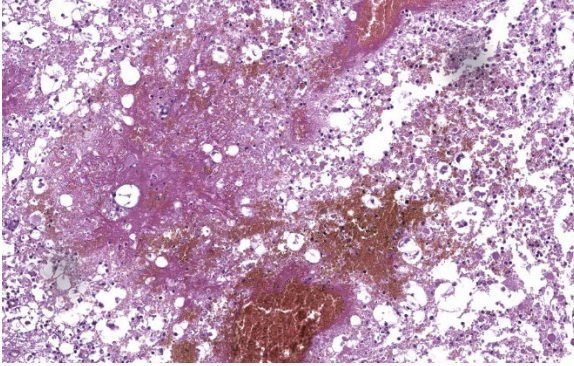


Figure 1-7. Spinal cord, cat. There is marked congestion and hemorrhage of vessels within the spinal cord. There is diffuse malacia of the gray and white matter with numerous spheroids. (HE, 169X)

Conference participants discussed the abundant ancillary changes in section, such as the polyphasic atrophy, degeneration, and regeneration present in the surrounding skeletal muscle. The history of hemilaminectomy at the site complicated analysis of these changes, making it difficult to determine which changes were due to surgical manipulation and which were caused by the pressure of the expansile vertebral angiomas.

Participants felt that the bone changes caused by the vertebral angiomas were significant and should be mentioned in the morphologic diagnosis. Participants also felt the morphologic diagnosis should acknowledge the hemilaminectomy that is an obvious feature of the section. Both were ultimately included in the morphologic diagnosis for this fascinating entity.

References:

1. Baron CP, Puntel FC, Fukushima FB, da Cunha O. Progressive cutaneous angiomas in the metatarsal region of a cat. *J Am Vet Med Assoc.* 2020;256(2):226-229.

2. Bulman-Felming J, Gibson T, Kruth S. Invasive cutaneous angiomas and thrombocytopenia in a cat. *J Am Vet Med Assoc.* 2009;234(3):381-384.
3. Corbett M, Kopec B, Kent M, Rissi DR. Encephalic meningoangiomas in a cat. *J Vet Diagn Invest.* 2022;34(5):889-893.
4. Belluzzi E, Caraty J, Vincken G, Esmens MC, Bongartz A. Vertebral angiomas recurrence in a 14-month-old Maine Coon cat. *Vet Rec Case Rep.* 2018;6(4):11-13.
5. Frizzi M, Ottolini N, Spigolon C, Bertolini G. Feline vertebral angiomas: two cases. *J Feline Med Surg Open Rep.* 2017;3(2): 205511691774412.
6. Gagliardo T, Pagano TB, Lo Piparo S, et al. Vertebral angiomas in a dog. *J Am Anim Hosp Assoc.* 2024;60(1):36-39.
7. Hans E, Dudley R, Watson A, et al. Long-term outcome following surgical and radiation treatment of vertebral angiomas in a cat. *J Am Vet Med Assoc.* 2018;253(12):1604-1609.
8. Jenkins T, Jennings R. Pulmonary capillary hemangiomas and hypertrophic cardiomyopathy in a Persian cat. *J Vet Diagn Invest.* 2017;29(6): 900-903.
9. Kipar A, Hetzel U, Armien A, Baumgartner W. Bilateral focal cerebral angiomas associated with nervous signs in a cat. *Vet Pathol.* 2001;38(3):350-353.
10. Kloc PA, Scrivani PV, Barr SC, et al. Vertebral angiomas in a cat. *Vet Radiol Ultrasound.* 2001;42(1):42-45.
11. Leonardi H, Poirier V, Iverson M, Samarini F. Successful long-term outcome with radiation and prednisolone following a postoperative feline vertebral angiomas relapse. *JFMS Open Rep.* 2023;9(1): 205511692311550.

12. Marr J, Miranda IC, Millder AD, Summers BA. A review of proliferative vascular disorders of the central nervous system of animals. *Vet Pathol.* 2021;58(5):864-880.
13. Meléndez-Lazo A, Ros C, de la Fuente C, Anor S, Fernandez-Flores F, Pastor F. What is your diagnosis? Vertebral mass in a cat. *Vet Clin Pathol.* 2017;46(1):185-186.
14. Ricco C, Bouvy B, Gomes E, Cauzinille L. Lumbar vertebral angiomatosis in a cat: a clinical case. *Revue Med Vet.* 2015;166(11): 332-335.
15. Schur D, Rademacher N, Vasanjee S, McLaughlin L, Gaschen L. Spinal cord compression in a cat due to vertebral angiomatosis. *J Feline Med Surg.* 2010;12(2): 179-182.
16. Wells M, Weisbrode S. Vascular Malformations in the Thoracic Vertebrae of Three Cats. *Vet Pathol.* 1987;24(4): 360-361.

CASE II:

Signalment:

Juvenile female sandhill crane (*Antigone canadensis*).

History:

The animal was presented to a local wildlife center with a cup attached to its beak. On initial exam, the submitting veterinarian noted emaciation, dehydration, and indentation on the beak as well as swelling of the right hock and left tibiotarsus, with no obvious abnormalities on radiographs. The bird was moved to an outside rehabilitation space 1 day after presentation and was eating and gaining weight reliably. The animal was found deceased a few weeks later.

Gross Pathology:

The animal weighs 2.2 kg and is in thin physical condition as evidenced by atrophied pectoral musculature and adipose tissue. There is a concentric deep indentation midway along the length of the beak. Overlying the right ankle are multiple firm, occasionally ulcerated nodules that are 2 to 5 mm in diameter. When sectioned the nodules are pale blue or tan, firm, and translucent with a botryoid appearance. Dissection of the joint shows many similar nodules firmly attached to the dermis, soft tissues, ligaments, and tendons. The condyle of the tibiotarsus has a fracture with pitting and marked proliferation of white firm nodules in the defect and epicondyle.

There is a focal, firm, nodular swelling overlying the distal left tibiotarsus that measures 1.8 cm x 0.8 cm. When sectioned, the nodule is tan and translucent. Relative to the right pectoral muscle, there is moderate wasting of the left pectoral musculature.

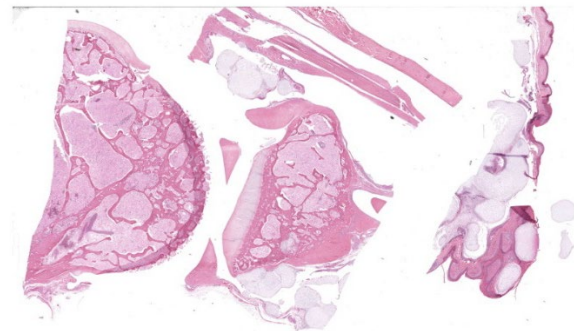


Figure 2-1. Tibiotarsal joint, sandhill crane. The joint is dissected. At lower left is the tibiotarsal joint, at top is the gastrocnemius tendon and sheath, and at right is the overlying skin. At subgross magnification, there are nodules of proliferating cartilage within the joint space, tendon sheath, and overlying dermis. (HE, 4X)

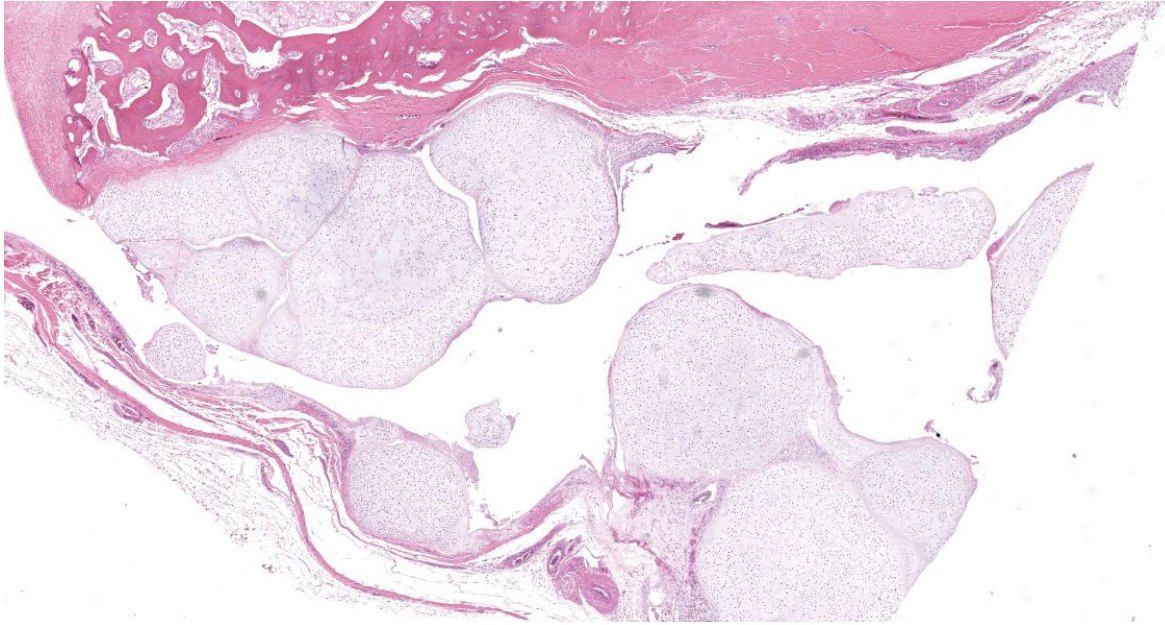


Figure 2-2. Tibiotarsal joint, sandhill crane. Arising from the joint capsule and lining the proximal tibia are nodules of cartilage measuring about 8mm in diameter. (HE, 23X)

Within the mid-trachea at the level of the reflexive curvature are multiple intraluminal trematodes. The organisms are 1.4 cm long, flat and fusiform with a bulbous anterior end; they are white with bilateral dark brown linear striations. Within the affected area, the tracheal mucosa is red and slightly thickened.

There are no significant gross abnormalities in the tongue, esophagus, lungs, heart, liver, spleen, pancreas, kidneys, proventriculus, ventriculus, small intestine, large intestine, or brain. The spinal cord is not examined in this case.

Microscopic Description:

Ankle joint: The bone profile is irregular due to many cartilage nodules that arise from the synovium of the joint spaces (synovium) and tendon sheaths (tenosynovium). Nodules contain many evenly spaced chondrocytes in hyaline pale blue matrix; they have moderate finely vacuolated pale purple cytoplasm and

large round nuclei with peripheralized chromatin and 1-3 nucleoli. Anisocytosis and anisokaryosis are marked. Mitoses are not evident. Binucleate cells are occasionally evident, and a trinucleate cell was seen. Many of the chondrocytes are pyknotic or karyolytic with pink cytoplasm (necrosis); such cells are dispersed between viable cells or predominate in the center of nodules where there is fragmentation of matrix and rarefaction of tissue. In larger nodules, the central chondrocytes cluster with intervening areas of acellular matrix. The synovium is thin and often necrotic when stretched over the nodules, with small thrombi in the associated vessels. In other areas the subintima is thickened by large mesenchymal cells embedded in mucinous matrix and variable numbers of lymphocytes, plasma cells, and heterophils. Scant fibrin and karyorrhectic cells are present in the joint spaces. The bone surfaces have mild remodeling, there is marked serous atrophy of marrow fat, and skeletal myocytes are atrophied.

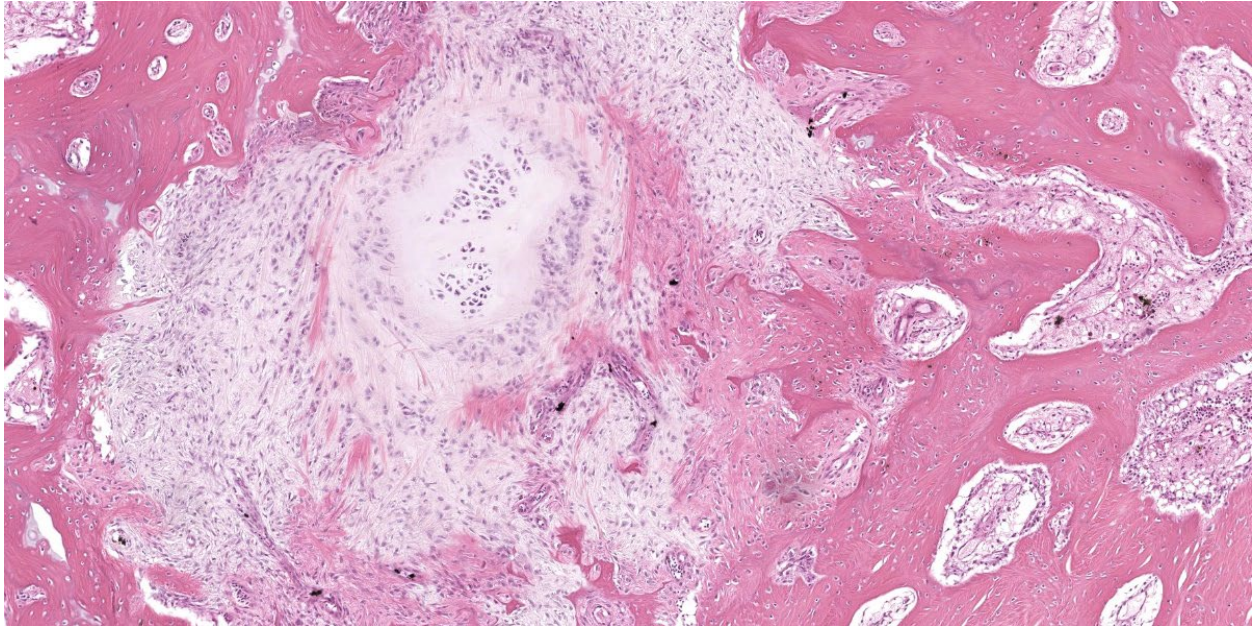


Figure 2-3. Tibiotarsal joint, sandhill crane. Proliferating mesenchymal cells within the tibial marrow space are giving rise to cartilage. (HE, 91X)

The skin bulges and is ulcerated due to several cartilage nodules in the subcutis, dermis, and epidermis. Synovium surrounds the intradermal nodules and merges with the inflamed and fibrotic dermis. Intraepidermal nodules are demarcated from the dermis by many heterophils; their cartilage matrix is pale blue to pink, and cells are pyknotic along the subcorneal surface. The epidermis overlying the intraepidermal nodules is necrotic and the surrounding epidermis is hyperplastic (acanthosis, increased mitoses). The stroma around and deep to the intraepidermal nodules is expanded by many red cells, heterophils, and compact collagen that has many fine karyorrhectic fragments, as well as small thrombosed vessels.

Contributor’s Morphologic Diagnoses:

1. Tibiotarsus: Moderate chronic heterophilic synovitis with synovial and tenosynovial chondromatosis

2. Skin: Multifocal chondromatosis with epidermal hyperplasia and necrosis, heterophilic dermatitis, and transepithelial elimination

Contributor’s Comment:

Synovial chondromatosis (also known as synovial chondrometaplasia) is an uncommon non-neoplastic process characterized by the formation of multiple cartilage nodules in synovial tissues of a joint, tendon sheath, or bursa. When the majority of these nodules undergo endochondral ossification, the term osteochondromatosis is used.^{2,3,7} Reports in animals have mostly been in dogs^{1,7,8,10,14} and raptors^{11,15,18} but horses and pigs can also be affected.^{6,13} It should be noted that osteochondromatosis of cats is different in its biological behavior, distribution, and possible etiology, and thus should not be combined when discussing the disease entity in other species.³ Males predominate in reports from both dogs and humans, while the few reports in raptors

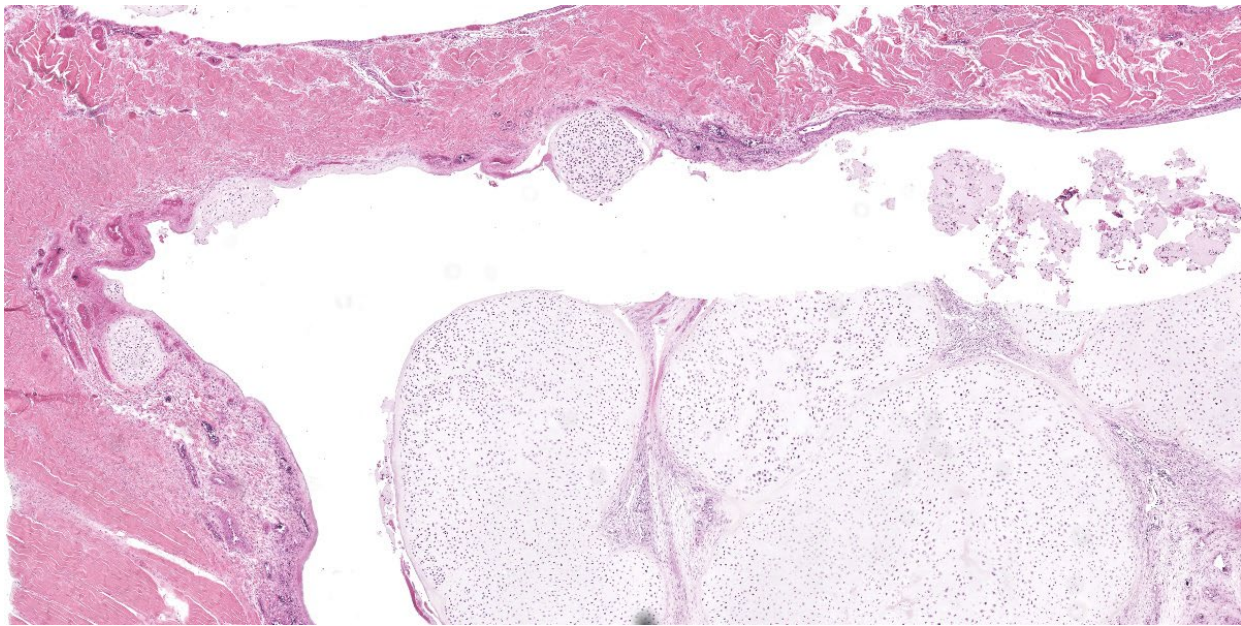


Figure 2-4. Tibiotarsal joint, sandhill crane. Nodules of cartilage arise within the tendon sheath (at left) and extend into the tendon sheath lumen (center). (HE, 39X)

have increased numbers of females.^{3,11,15,18} In dogs most reports are from large and giant purebreds from 7 months to 11 years old. The shoulder joint is most often affected, although cases have also been observed in the stifle, elbow, hock, and digits.^{2,3} Clinical signs include chronic progressive lameness with swelling of the joint.^{1,7,8,10}

In raptors, the majority of cases are reported bilaterally in the scapulohumeral joints of great horned owls (*Bubo virginianus*), with or without osteoarthritic change. Fewer cases of chondromatosis in the stifle joints have been reported.^{11,15,18} Birds often present in poor nutritional condition due to severe mobility restriction. This case is the first report of chondromatosis in the *Gruiformes* group and affecting the ankle joints.

Two forms of synovial chondromatosis (primary and secondary) have been described. Primary (idiopathic) chondromatosis occurs

spontaneously within the synovium of a single, otherwise unremarkable joint; it is rare in humans and animals. Grossly, primary synovial chondromatosis presents with more nodules than secondary chondromatosis.³ The pathogenesis of primary synovial chondromatosis is unknown, and it is thought to be an idiopathic nodular cartilaginous metaplasia of the synovium. Secondary chondromatosis is thought to be a reaction to a traumatic, degenerative, or inflammatory joint disease. Speculatively, the etiology in raptors is thought to be a chronic inflammatory process due to joint strain.¹⁵ In older horses and dogs, it is usually an incidental finding at necropsy, while in raptors it is often associated with the demise of the individual due to an inability to fly.^{3,15} Nodules are reported to be less numerous and mixed with other forms of synovial proliferation and metaplasia. Erosive changes in the articular cartilage are often more marked than the degree of synovial proliferation.³ In this case, the bilateral occurrence in the ankles,

presence of synovitis, and fracture of the tibiotarsus indicates secondary synovial chondromatosis.

Classically, gross lesions are described as multiple firm or hard white nodules embedded in the synovium and periarticular connective tissues, with variably intact articular cartilage.^{2,3,14} The nodules consist of islands of highly cellular hyaline cartilage covered by a layer of synoviocytes or fibrous tissue attached to or continuous with the synovial lining of joints or bursae. Chondrocytes may be haphazardly clustered, large, and sometimes binucleate. In this case, trinucleate chondrocytes were rarely evident. Areas of fibrocartilage, central necrosis, or endochondral ossification with medullary hematopoiesis may also be present. In some cases proliferative plasmacytic synovitis is reported.^{3,17} Nodules may detach from the synovium and float freely in the joint. In these cases, they are termed “loose bodies” and may undergo ischemic necrosis.^{2,12} Extra-articular chondromatosis has been rarely reported; in this case chondrometaplasia was evident in a tendon sheath.⁷

Under certain circumstances, nondermal elements enter the epidermis and are eliminated to the outside, a process termed ‘transepithelial elimination’ (TE).¹² Four subdivisions of TE are described, two of which involve large portions of tissue, as in our case (subdivisions 3 and 4). As migrating tissues compress the epidermis from below, epithelial damage occurs with necrosis and ulceration, and possible sloughing.¹² Transepithelial elimination, to the authors’ knowledge, has not been reported in association with synovial chondromatosis or in the class *Aves*. In this case, TE probably occurs as a result of the pressures exerted on the nodules by the relatively immobile and non-distensible skin of the ankle in birds. This

area may also have increased susceptibility to ulceration versus a more protected scapulo-humeral lesion, which is more often seen in birds with chondromatosis.

Differential diagnoses for synovial chondromatosis include chondroma and chondrosarcoma. Chondroma is a benign neoplasm of cartilage that has been occasionally reported in multiple veterinary species. Histologically, chondromas may have similar irregular lobules of hyaline cartilage, which may also have foci of endochondral ossification and mineralization. In fact, some report that primary chondromatosis may be a multifocal form of a chondroma.^{5,6} An important differential diagnosis is synovial chondrosarcoma. Malignant transformation of synovial chondromatosis to chondrosarcoma is rarely reported in dogs.^{1,7} Features that suggest chondrosarcoma are bone invasion and replacement of the chondrocyte cluster pattern with a more random distribution of cells.^{1,3,7}

Contributing Institution:

Veterinary Diagnostic Laboratory
University of Illinois at Urbana-Champaign
Urbana, IL
<https://vdl.vetmed.illinois.edu/>

JPC Diagnosis:

Joint capsule, tendon sheath, and overlying skin: Chondromatosis, nodular, multifocal, severe, with intra-osseous extension, transepithelial elimination, and chronic tenosynovitis and dermatitis.

JPC Comment:

The contributor provides an excellent summary of synovial chondromatosis (SC) as this photogenic entity presents in dogs, birds, pigs, and horses. Cats, however, long known for their flair for the idiosyncratic, have a similar

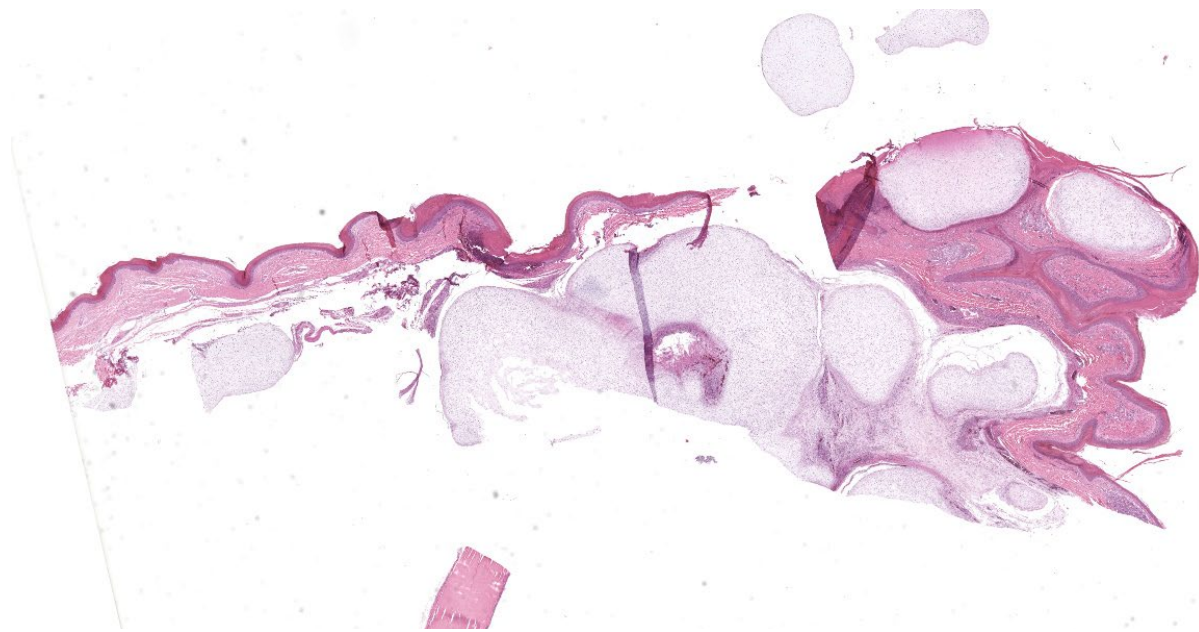


Figure 2-5. Tibiotarsal joint, sandhill crane. Nodules of cartilage are present within the dermis and extend to the epidermis (transepidermal elimination). (HE, 39X)

sounding but distinct condition, feline osteochondromatosis, which is distinct from the synovial chondromatosis discussed above and from osteochondromatosis in other animals.¹⁶ In horses, dogs, pigs, and humans, osteochondromatosis demonstrates an autosomal dominant inheritance pattern and typically occurs in young animals only during the period of active bone growth.¹⁶ The cartilage-capped tumors that arise from bone surfaces give the condition its name and tumor growth arrests once growth plates close.¹⁶

In contrast, feline osteochondromatosis usually presents in adult cats (most commonly 2-4 years old) long after skeletal maturity is achieved. The condition presents with no breed or sex predisposition and does not appear to be inherited. The disease affects the axial skeleton and, in a sad departure from the tumor arrest seen in other animals, tumors show progressive growth and can undergo malignant transformation to osteosarcoma or chondrosarcoma.¹⁶

Interestingly, feline osteochondromatosis is usually diagnosed in cats concurrently infected with feline leukemia virus (FeLV), leading to speculation that FeLV infected fibroblasts account for the special pathogenesis and distinct clinical behavior of osteochondromatosis in cats relative to other species.^{9,16} FeLV particles have been visualized within feline osteochondromatous tissue via electron microscopy and via in situ hybridization; however, a direct pathogenetic link between FeLV infection and the condition has not been conclusively established, and osteochondromatosis has been reported in FeLV-negative cats.^{9,16}

In humans, dogs, and a few cats, osteochondromatosis has been associated with premature stop codon-producing frameshift mutations in the exostosin glycosyltransferase 1 and 2 genes (EXT1 and EXT2, respectively), whose protein products form an enzyme complex that modifies heparan sulfate chains.⁴ It

is thought that heparan sulfate chain dysfunction can scramble chondrocyte differentiation or proliferation pathways, fibroblastic growth factors, bone morphogenic proteins, and Wnt signalling pathways, all of which could account for the lesions of osteochondromatosis.⁴ These theoretical pathogeneses have not been proven in human or in veterinary medicine, and in all species tested, EXT1 and EXT2 mutations are absent in a significant subset of osteochondromatosis cases.⁴

One such recent case report detailed the radiographic and pathologic findings of feline osteochondromatosis in an aged, 12-year-old Russian Blue, FeLV-negative cat with a years-long history of progressive forelimb lameness.⁹ Radiographs revealed bilateral, calcified proliferative lesions of the elbow joints and multiple vertebral bodies and ribs. Grossly, the elbow joints were completely ankylosed by large, round masses containing white material that replaced normal tissue architecture; the affected vertebrae and ribs contained similar lesions.⁹ Testing for EXT1 and EXT2 mutations and FeLV infection were all negative, confirming that this condition can arise spontaneously in aged cats.⁹

Back in the joints of the sandhill crane, the moderator noted that this, along with vertebral angiomas, was yet another entity with bland looking cells that nevertheless have no business being where they are. Conference participants noted the lack of anisocytosis, anisokaryosis, and mitotic figures, all of which point toward a benign process; however, the intra-osseous nodule of cartilage, which should not be present in a pure case of synovial chondromatosis, raised the spectre of chondrosarcoma for some participants. Participants ultimately decided that the bland histologic appearance of the cells likely precluded

chondrosarcoma diagnosis, but the phrase “with intra-osseous extension” was added to the morphologic diagnosis to capture this unusual feature.

References:

1. Aeffner F, Weeren R, Morrison S, Grundmann INM, Weisbrode SE. Synovial osteochondromatosis with malignant transformation to chondrosarcoma in a dog. *Vet Pathol.* 2012;49(6):1036-1039.
2. Craig LE, Dittmer KE, Thompson KG. Bones and Joints. In: Maxie MG, ed. *Jubb, Kennedy, and Palmer's Pathology of Domestic Animals.* 6th ed. Vol 1. 2016;Elsevier:161-163.
3. Craig LE, Thompson KG. Tumors of Joints. In: Meuten DJ, ed. *Tumors in domestic animals.* 5th ed. John Wiley & Sons Inc;2016:337-355.
4. D'Arienzo A, Andreani L, Sacchetti F, Colangeli S, Capanna R. Hereditary multiple exostoses: current insights. *Ortho Res Rev.* 2019;11:199-211.
5. Davis RI, Foster H, Arthur K, Trewin S, Hamilton PW, Biggart DJ. Cell proliferation studies in primary synovial chondromatosis. *J Pathol.* 1998;184(1):18-23.
6. de Brot S, Grau-Roma L, Vidal E, Segalés J. Occurrence of osteochondromatosis (multiple cartilaginous exostoses) in a domestic pig (*Sus scrofa domestica*). *J Vet Diagn Invest.* 2013;25(5):599-602.
7. Díaz-Bertrana C, Durall I, Rial JM, Franch J, Fontecha P, Ramis A. Extra- and intra-articular synovial chondromatosis and malignant transformation to chondrosarcoma. *Vet Comp Orthop Traumatol.* 2010;23(4):277-283.
8. Edinger DT, Manley PA. Arthrodesis of the shoulder for synovial osteochondromatosis. *J Small Anim Pract.* 1998;39(8):397-400.

9. Gomez A, Rodriguez-Largo A, Perez E, et al. Feline osteochondromatosis in a 12-year-old feline leukaemia virus-negative cat. *J Comp Pathol.* 2003;25:24-26.
10. Gregory SP, Pearson GR. Synovial osteochondromatosis in a labrador retriever bitch. *J Small Anim Pract.* 1990;31(11):580-583.
11. Howard MO, Nieves MA, Miles KG. Synovial chondromatosis in a great horned owl (*Bubo virginianus*). *J Wildl Dis.* 1996;32(2):370-372.
12. Mehregan AH, Hashimoto, K. General Pathology: Terminology. In *Pinkus' Guide to Dermatohistopathology* Appleton & Lange;1995:83-100.
13. Smith RK, Coumbe A, Schramme MC. Bilateral synovial chondromatosis of the metatarsophalangeal joints in a pony. *Equine Vet J.* 1995;27(3):234-238.
14. Smith TJ, Baltzer WI, Löhr C, Stieger-Vanegas SM. Primary synovial osteochondromatosis of the stifle in an English Mastiff. *Vet Comp Orthop Traumatol.* 2012;25(2):160-166.
15. Stone EG, Walser MM, Redig PT, Rings B, Howard DJ. Synovial chondromatosis in raptors. *J Wildl Dis.* 1999;35(1):137-140.
16. Szilasi A, Koltai Z, Denes L, Balka G, Mandoki M. In situ hybridization of feline leukemia virus in a case of osteochondromatosis. *Vet Sci.* 2022;9(2):59.
17. Villacin AB, Brigham LN, Bullough PG. Primary and secondary synovial chondrometaplasia: histopathologic and clinico-radiologic differences. *Hum Pathol.* 1979;10(4):439-451.
18. Xie S, Nevis J, Lezmi S. Pathology in practice. Chondro-osseous metaplasia consistent with synovial chondromatosis in a great horned owl. *J Am Vet Med Assoc.* 2014;245(7):767-769.

CASE III:

Signalment:

4-year-old male African pygmy hedgehog (*Atelerix albiventris*).

History:

This hedgehog presented to the teaching hospital for severe dental disease. A submandibular mass was noted during examination. Under anesthesia for a dental procedure, the animal decompensated, developing cyanosis. The patient showed clinical improvement when naloxone was administered and had a prolonged recovery from anesthesia. The patient was mobile and eating following recovery, but acutely decompensated 1.5 hours later. Resuscitation was attempted but was unsuccessful.

Gross Pathology:

The hedgehog was in good body condition. There was slight deviation of the muzzle to the right. Only one tooth (the lower right first incisor) remained in the dental arcade and was easily removed with traction. Both mandibles were mildly thickened and slightly irregular with smooth undulations noted in the gingiva. Mild hemorrhage was present near the right submandibular salivary gland and a 0.5 cm pale nodule (presumed enlarged lymph node) was associated with the gland. Dark pink discoloration and consolidation of the lung was present bilaterally and scattered, small (1 mm) white foci were noted in the affected regions. The heart weighed 1.8 g (0.56% of the total body weight).

Laboratory Results:

Light growth of *Neisseria animaloris* was isolated from the right submandibular lymph node (aerobic culture; species identified using MALDI-TOF). No microbial growth was isolated from this organ on anaerobic culture.

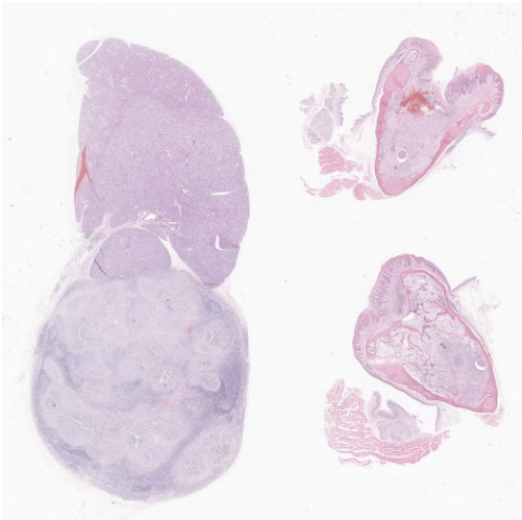


Figure 3-1. Lymph node and jaw, hedgehog. One section of mandibular lymph node and two sections of jaw are submitted for examination. At this magnification, 75% of the nodal architecture is effaced by an inflammatory infiltrate. (HE, 5X)

Microscopic Description:

Submandibular lymph node: Large coalescing regions of pallor obscure the normal architecture of the enlarged lymph node. Areas of pallor consist of multifocal to coalescing nodular aggregates of mostly neutrophils with fewer epithelioid macrophages, lymphocytes, plasma cells, eosinophils, and multinucleated giant cells. At the center of the infiltrates are frequent deposits of basophilic bodies occasionally with peripheralized eosinophilic acellular material (Splendore-Hoeppli reaction). Small, non-filamentous, coccoid Gram-negative bacteria are identified at the center of these deposits using a Gram stain. At the periphery of the cell aggregates, there are thin concentric bands of connective tissue and moderate eosinophilic infiltrates. A few small scattered secondary lymphoid follicles are separated by sheet like infiltrates of plasma cells.

Jaw: There are multifocal to coalescing regions of increased cellularity and loss of trabecular bone within the mandible. Cellular infiltrates consist of nodular aggregates of mostly neutrophils with fewer epithelioid macrophages, lymphocytes, plasma cells, and rare eosinophils and multinucleated giant cells. At the center of the infiltrates are rare radiating deposits of basophilic material with peripheralized eosinophilic acellular material (Splendore-Hoeppli reaction). At the periphery of the cell aggregates, there are thin concentric bands of connective tissue, plasma cell infiltrates, and focal hemorrhage. Remodeling of the surrounding bone with new woven bone formation is evident. The gingival mucosal epithelium is hyperplastic, eroded, and infiltrated by neutrophils and fewer eosinophils.

Contributor's Morphologic Diagnoses:

1. Submandibular lymph node: Lymphadenitis, pyogranulomatous, multifocal to coalescing, chronic, severe, with intralesional Gram-negative bacteria and Splendore-Hoeppli reaction.
2. Jaw: Osteomyelitis, pyogranulomatous, multifocal to coalescing, chronic, severe, with intralesional bacteria and Splendore-Hoeppli reaction.

Contributor's Comment:

This hedgehog had a history of significant dental disease resulting in loss/removal of most of the teeth. Dental diseases, including gingivitis, periodontitis, tooth fracture, tooth loss, excess dental wear, dental abscesses, and even oral osteomyelitis are common in this species.^{1,6} Mandibular osteomyelitis was marked and was accompanied by a similar reaction in the draining lymph node and in the lung (not included in the submission). Splendore-Hoeppli phenomenon was evident within the lesions. This nonspecific reaction is

thought to reflect the deposition of antigen-antibody complexes and inflammatory cell products/debris, and occurs around clusters of microorganisms, such as bacteria and fungi, or biologically inert substances.⁵ Genera of bacteria that are commonly associated with this reaction include *Actinomyces*, *Nocardia*, *Staphylococcus*, *Streptococcus*, *Proteus*, *Pseudomonas*, and *Escherichia coli*.⁵

Mandibular osteomyelitis is not uncommon as a cause of morbidity in pet and wild hedgehogs and may occur secondary to periodontitis, but there are few studies confirming the etiology of these lesions.^{6,7,10} In mortality studies on European hedgehogs (*Erinaceus europaeus*), mandibular abscesses and botryomycosis were detected in 23% of evaluated animals but these lesions were reportedly confined to the submandibular soft tissues, and they were not evaluated microbiologically.¹⁰

The lesion in this hedgehog has a similar appearance to “lumpy jaw” resulting from *Actinomyces bovis* infections in cattle, and a similar lesion has been described in a captive African pygmy hedgehog infected with *Actinomyces naeslundii*.^{7,8} Like the reported case, there was involvement of the draining lymph node and the lung in this hedgehog. However, the bacterium in the submitted case was Gram-negative and pure growth of *Neisseria animaloris* was isolated from the lesion.

Neisseria animaloris is a common inhabitant of the oral cavity of animals (particularly cats and dogs) and may cause systemic infections in humans and animals, often as a result of a bite wound.^{2,3,4} These infections can result in localized or systemic pyogranulomatous lesions which exhibit Splendore-Hoeppli reaction around the Gram-negative diplococci.^{2,3} Given the zoonotic potential of this bacterium,

it would be interesting to know if this organism is part of the normal oral microbiome of the African pygmy hedgehog.^{3,4} If so, this may add to the growing list of known zoonotic bacterial pathogens potentially carried by captive and wild hedgehogs, which already includes *Leptospira* spp., *Salmonella* spp., *Mycobacterium* spp, methicillin-resistant *Staphylococcus aureus*, and *Streptococcus* spp.⁹

While the oral lesions in this case were considered significant, cyanosis during anesthesia and the subsequent death of this patient was most likely due to heart failure resulting from cardiomyopathy.

Contributing Institution:

Atlantic Veterinary College
University of Prince Edward Island
Department of Pathology and Microbiology
<https://www.upei.ca/avc/pathology-and-microbiology>

JPC Diagnoses:

1. Lymph node: Lymphadenitis, pyogranulomatous, diffuse, marked, with Splendore-Hoeppli material and colonies of cocci.
2. Mandible: Osteomyelitis, pyogranulomatous, diffuse, marked, with pathologic fracture, ulcerative and lymphoplasmacytic gingivitis, Splendore-Hoeppli material, and colonies of cocci.



Figure 3-2. Lymph node, hedgehog. Nodal architecture is effaced by numerous poorly demarcated pyogranulomas. (HE, 111X)

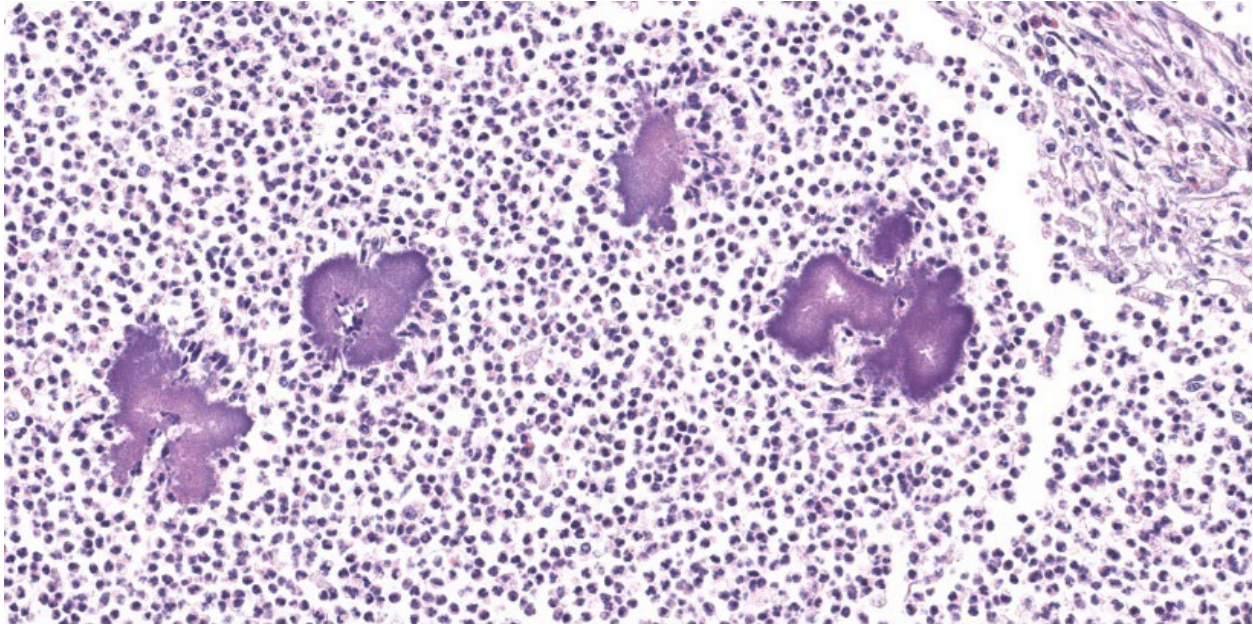


Figure 3-3. Lymph node, hedgehog. Pyogranulomas are centered on colonies of cocci enmeshed in Splendore-Hoeppli material. (HE, 337X)

JPC Comment:

The contributor provides an excellent case of mandibular osteomyelitis in an African hedgehog which highlights the tendency of this species to develop pathology in the oral cavity. African hedgehogs are short-lived exotic pets with a life expectancy of 4 to 6 years and are considered geriatric at 3-5 years of age.⁶ They are particularly prone to neoplasia, even in early age, and are susceptible to age-related cardiovascular, renal, and periodontal disease.⁶

Hedgehogs are particularly prone to dental disease, including gingivitis, dental calculus, periodontitis, and tooth loss.⁶ Periodontal disease may be preventable with proper diet, with dry kibble and raw fruits and vegetables thought to promote periodontal health versus moist or canned foods.⁶ Hedgehog oral disease of any variety may be accompanied by florid gingival hyperplasia that can be difficult to distinguish from neoplasia grossly. Clinical signs include

reduced food intake or changes in food preferences, anorexia, weight loss, dysphagia, drooling, hemorrhage, and halitosis.⁶ Gross findings may include gingival swelling and inflammation, loose or missing teeth, swelling of the face, and abnormal facial bone positioning.⁶

Oral squamous cell carcinoma (SCC) is the most common tumor of the African hedgehog digestive system and is reported to be the most common overall hedgehog neoplasia.⁶ Oral SCC has been reported in hedgehogs as young as 1 year old and as old as 6 years. Diagnosis can be difficult without histology as the cytologic appearance of oral SCC needle aspirates can look very similar to early stage periodontal disease, and distinguishing the two conditions on cytology alone is often impossible.⁶ Surgical excision of oral tumors, including SCC, is often incomplete and oral tumors frequently recur; prognosis is therefore poor for oral neoplasia, making differentiating between oral neoplasia and periodontal disease,

which often responds well to targeted antimicrobial therapy, of prime prognostic importance.⁶

The aged hedgehog in this case read the textbook, with severe oral and cardiovascular disease at the time of death. Conference participants noted the large peripheral nerve surrounded by the intense inflammatory milieu and spared a thought for what must have been an extremely painful condition for this hedgegie. The moderator encouraged participants to evaluate bone at the subgross level where symmetry is most easily assessed. Subgross evaluation in this case reveals an extremely unsymmetrical mandible, which is an initial indication of bone involvement. The moderator also noted that polarization at subgross magnification can reveal which bone is well-organized parent bone and which is reactive. Subgross evaluation also reveals impressive gingival ulceration, which presumably provided an excellent portal for *Neisseria animaloris* to enter the deeper tissue of the oral cavity and provoke the incredible inflammatory response captured on this delightful slide.

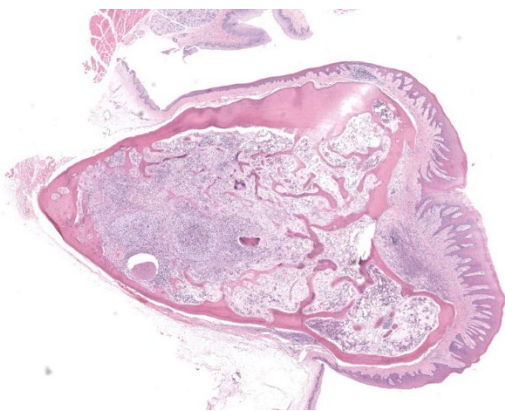


Figure 3-4. Mandible, hedgehog. There are similar pyogranulomas within the medullary cavity of the mandible. (HE, 18X)

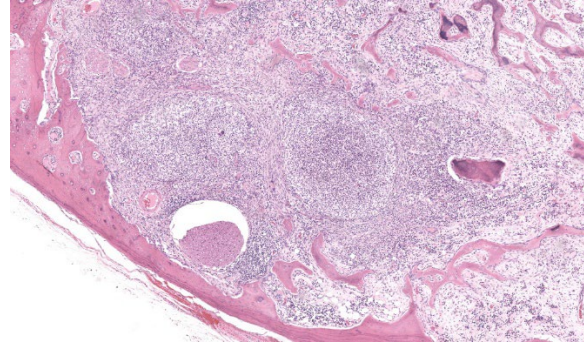


Figure 3-5. Mandible, hedgehog. There is marked resorption of medullary and, to a lesser extent, cortical bone with pyogranulomatous inflammation. (HE, 57X)

Conference participants noted the somewhat unexpected abundance of eosinophils in the inflammatory infiltrate, which some participants noted was an occasional feature of inflammation in hedgehogs. This led to a brief discussion of eosinophilic leukemia, a myelogenous leukemia of hedgehogs that appears in middle age and carries a grave prognosis.

Participants felt that the morphologic diagnosis should include elements critical to the pathogenesis, which in this case is presumed to begin with ulcerative gingivitis, bacterial invasion, and pyogranulomatous inflammation. Participants also interpreted the appearance of the submucosal bone fragments under polarized light as pathologic fracture, which all thought warranted mention in the morphologic diagnosis.

References:

1. Chaprazov T, Dimitrov R, Yovcheva KS, Uzunova K. Oral and dental disorders in pet hedgehogs. *Turk J Vet Anim Sci.* 2014; 38(1):1-6.
2. Foster G, Whatmore AM, Dagleish MP, et al. Forensic microbiology reveals that *Neisseria animaloris* infections in harbour porpoises follow traumatic injuries by grey seals. *Sci Rep* 2019;9(1):14338.

3. Helmig KC, Anderson MS, Byrd TF, Aubin-Lemay C, Moneim MS. A rare case of *Neisseria animaloris* hand infection and associated nonhealing wound. *J Hand Surg Glob Online* 2020;2(2):113-115.
4. Heydecke A, Andersson B, Holmdahl T, Melhus A. Human wound infections caused by *Neisseria animaloris* and *Neisseria zoodegmatidis*, former CDC Group EF-4a and EF-4b. *Infect Ecol Epidemiol*. 2013;3:1-5.
5. Hussein MR. Mucocutaenous Splendore-Hoepli phenomenon. *J Cutan Pathol* 2008;35(11):979-988.
6. Johnson DH. Geriatric Hedgehogs. *Vet Clin North Am Exot Anim Pract*. 2020; 23(3):615-637.
7. Martinez LS, Juan-Salles C, Cucchi-Stefanoni K, Garner MM. *Actinomyces naeslundii* infection in an African hedgehog (*Atelerix albiventris*) with mandibular osteomyelitis and cellulitis. *Vet Rec* 2005; 157(15):450-451.
8. Olson EJ, Dykstra JA, Armstrong AR, Carlson CS. Bones, joints, tendons and ligaments. In: Zachary JF, ed. *Pathologic Basis of Veterinary Disease*. 7th ed. Elsevier; 2022:1037-1490.
9. Ruszkowski JJ, Hetman M, Turlewicz-Podbielska H, Pomorska-Mól M. Hedgehogs as a potential source of zoonotic pathogens-a review and an update of knowledge. *Animals (Basel)* 2021;11(6): 1754.
10. Zacharopoulou M, Guillaume E, Coupez G, Bleuart C, Le Loc'h G, Gaide N. Causes of mortality and pathological findings in European hedgehogs (*Erinaceus europaeus*) admitted to a wildlife care centre in southwestern France from 2019 to 2020. *J Comp Pathol*. 2022;190:19-29.

CASE IV:

Signalment:

3-month old male Sprague Dawley rat (*Rattus norvegicus*).

History:

The mother of this rat was injected with valproic acid at 12 days gestation (animal model of autism). All of the pups in that litter had kinks in their tails.

Gross Pathology:

A 12 cm amputated tail was submitted in formalin. Three centimeters proximal to the tip, the tail is bent at an angle of approximately 270 degrees with a subtler bend 1 cm from the tip.

Microscopic Description:

Examined are three longitudinal sections of the tail (skin removed). One section is composed mostly of muscle. In the other sections, two normal caudal vertebrae flank a malformed vertebra. In the middle section, the linear arrangement of the caudal vertebra is distorted by a small, eccentric, round to wedge-shaped bone containing a curved physis with somewhat disordered maturation of chondrocytes. The direction of chondrocyte maturation is oriented away from the midline of the tail. Medial to the physis is a layer of woven bone that is thicker at the periphery and thinner in the middle (osseous endplate) which blends with a layer of cartilage (cartilaginous end plate). Connecting to the periphery of the osseous endplate are laminar bands of collagen and fibroblasts which also connect to the adjacent vertebral body osseous endplates (annulus fibrosus). The annulus fibrosus also connects the osseous endplates of the cranial and caudal vertebrae and surrounds two foci of

chondrocytes, amorphous amphophilic material (proteoglycans), and large vacuolated cells (nucleus pulposus cells). These two foci are separated by a band of the annulus fibrosus which connects to the center of the cartilaginous endplate of the abnormal vertebra. The changes in the other section are similar, except there are bilateral abnormal vertebral segments which are connected to one of the adjacent vertebrae by woven bone and separated from the other adjacent vertebra by a band of annulus fibrosus. The two bony segments are separated by a central pocket of nucleus pulposus cells and proteoglycans. The physis of one of the adjacent vertebrae blends with the central nucleus pulposus, bisecting the osseous and cartilaginous end plates.

Contributor’s Morphologic Diagnosis:

Caudal vertebrae: Multifocal vertebral malformations (hemivertebra and butterfly vertebra).



Figure 4-1. Tail, rat. This is a littermate of the rat submitted for examination. The tail has two angular deformities. (Photo courtesy of: Virginia-Maryland College of Veterinary Medicine, <https://vetmed.vt.edu/>)

Contributor’s Comment:

The vertebrate tail is made up of between 2 (Manx cat) and 49 (long-tailed pangolin) caudal (or coccygeal) vertebrae. In tailless animals, the greatly reduced caudal vertebrae are fused to form the coccyx. The cranial-most caudal vertebrae have a well-developed vertebral arch with spinous and transverse processes. The vertebral canal contains the filum terminale and a variable number of caudal spinal nerve roots which exit the canal through the corresponding intervertebral foramina. The vertebrae toward the tip of the tail have a much simpler, cylindrical shape.

The intervertebral disc forms a fibrocartilaginous joint between adjacent caudal vertebrae. The intervertebral disc consists of a central nucleus pulposus surrounded by a tough annulus fibrosus. The nucleus pulposus is composed of water, type II collagen, proteoglycans, and nucleus pulposus cells. The large, vacuolated nucleus pulposus cells of young animals, similar to the notochordal cells (physaliferous cells) from which the disc is derived, are replaced by smaller, chondrocyte-like cells in adults.² The annulus fibrosus is composed of type I collagen and fibrocartilage arranged in laminae that attach to the osseous endplates of two adjacent vertebral bodies and provide resistance to tensile forces on the spine. The osseous endplate has a strong, solid, peripheral epiphyseal rim and a central portion made of thin, porous bone.¹¹ The intervertebral disc is separated from the cortical bone of the vertebral endplate by a thin layer of hyaline cartilage, type II collagen, and proteoglycans called the cartilaginous endplate.⁸ The dorsal and ventral boundaries of the intervertebral disc are the dorsal and ventral longitudinal ligaments.

Tail kinks can be caused by fracture with malunion or by congenital malformations.

Congenital malformations can be further divided into genetic diseases and teratogenic effects during development of the vertebral column. Genetic tail kinks are common in dogs and cats, especially in dog breeds such as Bulldogs, Boston Terriers, and Pugs.³ Embryologic development of the vertebral column begins with segmentation of the paraxial mesoderm on each side of the neural tube into somites. Next, each somite is divided into a ventral sclerotome, the precursor for the vertebrae, and a dorsal dermomyotome, which develops into the skeletal muscle and dermis of the back. The ventral sclerotome subunits fuse in cranial-caudal pairs as well as across the midline to form the vertebral body and the vertebral arch which encloses the developing spinal cord. Development and chondrification of the vertebrae precedes in an cranial to caudal direction, while the progression of ossification is less orderly.¹

Congenital vertebral malformations have been classified into either failure of segmentation, where the mesoderm does not properly divide into somites, leading to the appearance of vertebral fusion, or failure of vertebral formation, where elements of an individual vertebra do not form, leading to abnormally shaped vertebrae (wedge, hemi-, or butterfly vertebrae). Either type of deformity can lead to scoliosis (lateral deviation of the vertebral column) or kyphosis (dorsoventral deviation of the vertebral column). These defects have been classified based on which part (dorsal, lateral, or median) of the developing vertebra is deficient and whether the deficiency is complete (aplasia; hemivertebra) or incomplete (hypoplasia; wedge vertebra).³ A butterfly vertebra is caused by failure of the two lateral portions of the sclerotome to fuse across midline.⁵ These malformations can be further classified as segmented (separated from the adjacent vertebrae

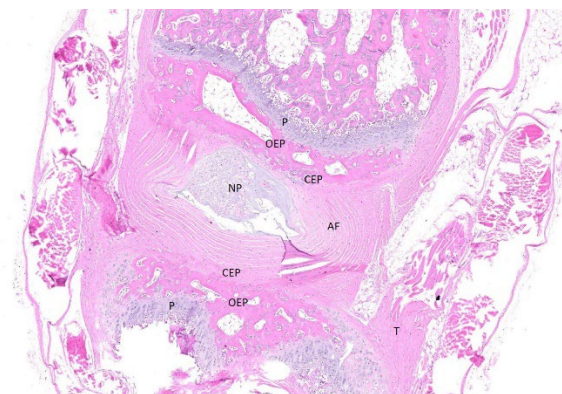


Figure 4-2. Tail, rat. Normal caudal vertebrae and intervertebral disc. (P = physis; OEP = osseous endplate; CEP = cartilaginous endplate; AF = annulus fibrosus; NP = nucleus pulposus; T = tendon.)

by intervertebral discs), nonsegmented (attached to the adjacent vertebrae by bone), or semi-segmented (attached to one adjacent vertebra by bone and separated from the other by an intervertebral disc). A typical vertebra has three centers of ossification (one in the body and one on each side of the arch) and four physes (one at each endplate and one on each side where the vertebral arch joins the body).¹ Since most caudal vertebrae lack arches, they have just the caudal and cranial physes. Based on the single longitudinal sections of this rat's tail, the defects are consistent with a segmented hemivertebra and a butterfly vertebra; however, two view radiographs, MRI, or serial sections would be needed to confirm the diagnosis.

Valproic acid is a short chain fatty acid used to treat epilepsy, migraine, and bipolar disorder. Actions of the drug include modulation of neurotransmission and epigenetic regulation of gene expression. In humans, prenatal exposure to valproic acid has been associated with an increased risk of autism spectrum disorders, as well as a variety of congenital malformations.⁹ Rodents exposed to valproic acid in utero are used as an animal model of autism.⁶

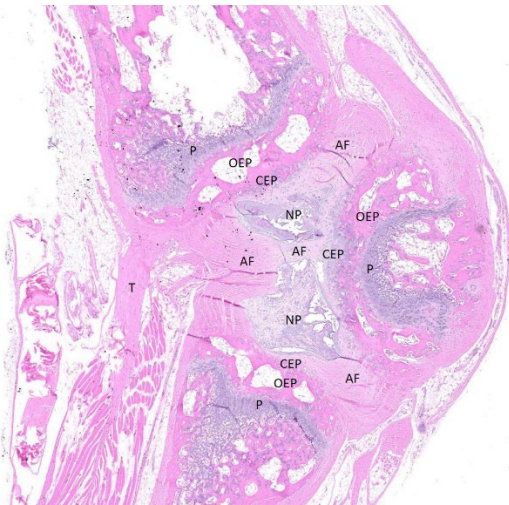


Figure 4-3. Tail, rat. Hemivertebra. (P = physis; OEP = osseous endplate; CEP = cartilaginous endplate; AF = annulus fibrosus; NP = nucleus pulposus; T = tendon.)

Although the exact pathogenesis is not known, proposed mechanisms of action for valproic acid-induced malformations include intracellular acidification, changes in lipid, zinc, folate, or retinoid metabolism, and alterations in developmental gene expression.⁹

Contributing Institution:

Virginia-Maryland College of Veterinary Medicine
Blacksburg, VA
<https://vetmed.vt.edu/>

JPC Diagnosis:

Tail: Vertebral malformation, multisegmental, with hemi- and butterfly vertebra formation.

JPC Comment:

As the contributor notes, the development of the vertebral column is complex, with the vertebral bodies forming from proliferating and migrating sclerotomes that surround the embryonic notochord.⁴ This complex process is orchestrated via spatially and temporally dis-

crete gene expression and cell signaling cascades that shape and position each vertebra in the proper cranial-caudal orientation.⁴

Even the most casual of anatomist will notice the segmental nature of the vertebrate spine and the different vertebral morphologies displayed at different levels of the spinal column. These patterning differences develop under the influence of *Hox* genes, which have been extensively studied in mice.⁷ Researchers have painstakingly mapped the *Hox* genes to particular functions, finding, for instance, that *Hox10* expression deactivates the rib-forming program in non-thoracic ribs and, when expression is experimentally blocked, lumbar vertebrae grow ribs.⁷ In snakes, *Hox10* genes have lost the ability to block rib formation, leading to rib growth down the entire length of the animal.⁷

Sonic hedgehog (Hh) signaling is another critical player in embryonic patterning and development. While Hh signaling is broadly important in the development of the face, skull, limbs, and axial skeleton, in the vertebral column, Hh signaling from the notochord is crucial in initial somite formation and the development and maintenance of intervertebral discs in development; in post-natal life, when the notochord becomes the nucleus pulposus, Hh signaling is key for the maintenance of intervertebral disc integrity.^{4,10}

These two patterning pathways are just two among many, and any missteps in this complex developmental dance produce congenital defects in the formed vertebra. This case nicely demonstrates, and the contributor nicely describes, two such morphologic defects, but there are many others. In humans, aberrant expression of *Hox* and/or Hh signaling have been associated with a syndrome

clunkily named VACTERL, for vertebral anomalies (V), anal atresia (A), cardiac malformation (C), tracheoesophageal fistula (TE), renal dysplasia (R), and limb abnormalities (L).⁴ This clinical syndrome is diagnosed when a patient has three or more of the listed abnormalities, and among the listed defects, vertebral abnormalities are found in up to 95% of patients.⁴ Perhaps a more familiar consequence of vertebral developmental defects is spina bifida, a congenital anomaly in which the vertebral arch fails to fuse. While the underlying pathogenesis have not been fully worked out, there is mounting evidence that abnormal *Hox* gene expression is the root cause of a number of neural tube defects, including anencephaly, spina bifida, hydrocephaly, and encephalocele.¹²

The complications of developmental anatomy were well illustrated on the histologic slide examined in conference. The moderator began by noting that the first location clue in this challenging slide is the prominent nucleus pulposus surrounded by the concentric rings of the annulus fibrosus. These features definitively localize the tissue to the vertebral column. In a rat, the nucleus pulposus should be a discoid shape and the affected vertebral joints in section feature very distorted architecture, indicating that the lesion is architectural and, therefore, likely developmental. The moderator agreed with the contributor that the exact nature of the vertebral malformations would be best assessed via advanced imaging, but that hemivertebra and butterfly butterfly formation were most likely based on the histologic features.

A common thread in this week's conference discussion was the perceived difficulty of evaluating bone pathology. In her closing

thoughts, the moderator challenged that assertion with the view that bone responds to injury in a stereotypic manner. The key to under

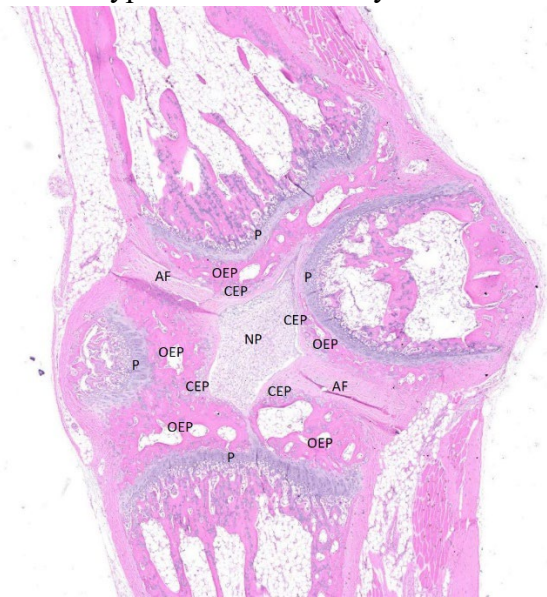


Figure 4-4. Tail, rat. Butterfly vertebra (C). (P = physis; OEP = osseous endplate; CEP = cartilaginous endplate; AF = annulus fibrosus; NP = nucleus pulposus; T = tendon.)

standing bone pathology, then, is understanding how bone behaves normally; once one understands how bone develops and how it undergoes modeling and remodeling in response to injury, then the pathology that you see can be essentially reverse engineered to narrow down the universe of potential pathologic insults.

Discussion of the morphologic diagnosis was mercifully straightforward with this case. Participants preferred to call the distribution multisegmental to emphasize that multiple vertebrae were affected, but the contributor's diagnosis was otherwise adopted largely intact.

References:

1. Burbidge HM, Thompson KC, Hodge H. Post natal development of canine caudal cervical vertebrae. *Res Vet Sci.* 1995;59 (1):35-40.

2. Chen S, Fu P, Wu H, Pei M. Meniscus, articular cartilage and nucleus pulposus: a comparative review of cartilage-like tissues in anatomy, development, and function. *Cell Tissue Res.* 2017;370(1):53-70.
3. Gutierrez-Quintana R, Guevar J, Stalin C, Faller K, Yeaman C, Penderis J. A proposed radiographic classification scheme for congenital thoracic vertebral malformations in brachycephalic “screw-tailed” dog breeds. *Vet Radiol Ultrasound.* 2014; 55(6):585-591.
4. Kalamchi L, Valle C. Embryology, Vertebral Column Development. StatPearls Publishing; 2024. Available at <https://www.ncbi.nlm.nih.gov/books/NBK549917>.
5. Katsuura Y, Kim HJ. Butterfly vertebrae: a systematic review of the literature and analysis. *Glob Spine J.* 2019;9(6):666-679.
6. Mabunga DFN, Gonzales ELT, Kim J, Kim KC, Shin CY. Exploring the validity of valproic acid animal model of autism. *Exp Neurol.* 2015;24(4):285-300.
7. Mallo M, Wellik DM, Deschamps J. Hox genes and regional patterning of the vertebrate body plan. *Dev Biol* 2010;344(1): 7-15.
8. Moon SM, Yoder JH, Wright AC, Smith LJ, Vresilovic EJ, Elliott DM. Evaluation of intervertebral disc cartilaginous endplate structure using magnetic resonance imaging. *Eur Spine J.* 2013;22(8):1820-1828.
9. Padmanabhan R, Abdulrazzaq YM, Bastaki SMA. Valproic acid-induced congenital malformations: Clinical and experimental observations. *Congenit Anom.* 2000;40(4):259-268.
10. Rajesh D, Dahia CL. Role of sonic hedgehog signaling pathway in intervertebral disc formation and maintenance. *Curr Mol Biol Rep.* 2018;4(4):173-179.
11. Wang Y, Battié MC, Videman T. A morphological study of lumbar vertebral endplates: radiographic, visual and digital measurements. *Eur Spine J.* 2012;21(11): 2316-2323.
12. Yu J, Wang L, Pei P, et al. Reduced H2K27me3 leads to abnormal *Hox* gene expression in neural tube defects. *Epigenetics Chromatin.* 2019;12:76.